論文 / 著書情報
Article / Book Information

Title	Wavelength Trimming of MEMS VCSELs for Post-process Wavelength Allocation
Author	Hayato Sano, Norihiko Nakata, Akihiro Matsutani, Fumio Koyama
Journal/Book name	, , ThA1-5, pp. 397-400
Issue date	2010, 6
DOI	http://dx.doi.org/10.1109/ICIPRM.2010.5516225
URL	http://www.ieee.org/index.html
Copyright	(c)2010 IEEE. Personal use of this material is permitted. Permission from IEEE must be obtained for all other users, including reprinting/republishing this material for advertising or promotional purposes, creating new collective works for resale or redistribution to servers or lists, or reuse of any copyrighted components of this work in other works.
Note	このファイルは著者（最終）版です。 This file is author (final) version.

Wavelength Trimming of MEMS VCSELs for Post-process Wavelength Allocation

Hayato Sano, Norihiko Nakata, Akihiro Matsutani and Fumio Koyama

Microsystem Research Center, Tokyo Institute of Technology, Japan

Email: sano.h.ab@m.titech.ac.jp

Abstract

We demonstrate the wavelength trimming of MEMS VCSELs by etching the cantilever-shaped top mirror using FIB. This technique can be used for the post-process precise wavelength allocation of athermal MEMS VCSELs. Experimental results show a possibility of realizing both red-shift and blue-shift wavelength changes by choosing the etching area of the cantilever.

1. Introduction

Vertical cavity surface emitting lasers (VCSELs) have been attracting great interest as light sources with low power consumption and small footprint. For further increase in transmission capacity even for short reach links, wavelength division multiplexing (WDM) should be considered. The temperature dependence of semiconductor lasers, which is typically 0.1nm/K for single-mode VCSELs, is a remaining problem to be solved. The elimination of costly thermoelectric controllers is needed for use in low cost WDM networks. If we are able to realize athermal semiconductor lasers exhibiting a fixed wavelength under temperature changes, we expect low power consumption and small packaging in WDM transmitter modules. Tunable VCSELs with micro electro mechanical system (MEMS) have been studied intensively [1-6]. We reported the athermal operation of 1550nm VCSELs with a thermally actuated cantilever based on bimorph effect [7-10]. In addition we present the first demonstration of the athermal and tunable operations of 850nm VCSELs with a newly designed MEMS cavity [11,12]. The athermal operation could be improved by inserting Al_xO_y anti-reflection layer in the cavity. We obtained the extremely low temperature dependence of 0.002nm/K.

Also, the post-process wavelength adjustment, so-called "wavelength trimming" [13], is needed in such athermal VCSELs for precise wavelength allocation. However the wavelength of athermal VCSELs cannot be controlled with a thermoelectric controller due to their athermal nature. We would like to point out a possibility to change the wavelength by modifying MEMS structure. The cantilever-shaped top distributed Bragg reflector (DBR) can be modified by dry etching, which results in wavelength shifts even after the fabrication. This trimming technique enables the presice wavelength allocation.

In this paper, we demonstrate the wavelength trimming of micromachined GaAs-based VCSELs by post-process etching of a cantilever structure.

2. Design of Athermal MEMS VCSELs

Figure 1 shows the cross-sectional view and scanning electron microscope (SEM) image of the fabricated MEMS VCSEL. The device consists of a top AlGaAs MEMS mirror, an active region including three GaAs/AlGaAs quantum wells and an AlGaAs bottom p-type DBR including an oxide

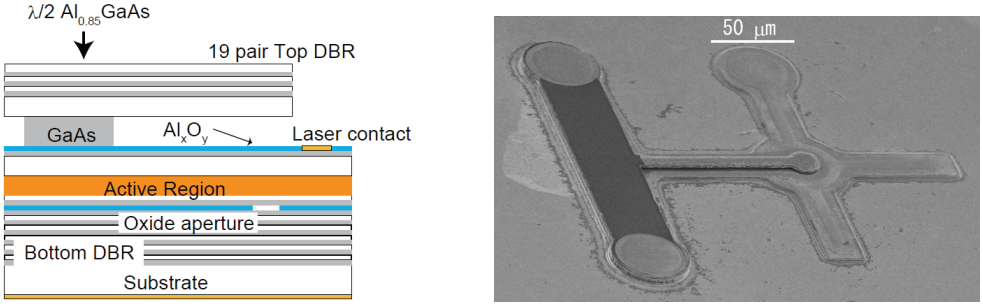

Fig. 1: The schematic and SEM image of the fabricated MEMS VCSEL for wavelength trimming

aperture, which provides optical and electrical confinement. The top MEMS mirror is a freely suspended cantilever-shaped AlGaAs n-DBR including a 4λ-thick (1.1 μm) $Al_{0.85}Ga_{0.15}As$ stress-control layer at the bottom. The thermal expansion coefficient of the strain control layer is smaller than the average one of DBR. Because of different thermal expansion coefficients in GaAlAs compositions, we are able to obtain the thermal actuation of the cantilever for compensating the temperature dependence of wavelength. The air gap is formed (or the cantilever is released) by selective etching of a GaAs sacrificial layer underneath the cantilever. A similar concept using a stress-induced displacement of the cantilever can be used for wavelength trimming. Because there is an internal stress in the cantilever resulting from different lattice constants in different AlGaAs compositions, we are able to obtain the displacement of the cantilever when it is released. Thus, the displacement changes the air-gap length and hence the lasing wavelength. We can increase or decrease the displacement by controlling the internal stress with dry etching after forming the air-gap.

We newly inserted the Al_xO_y layer which functions as anti-reflection coating. The Al_xO_y layer was formed by using the wet oxidation of $Al_{0.98}Ga_{0.02}As$. In the case of conventional MEMS VCSELs, the wavelength control can be realized by changing the air gap. In order to enhance the tuning efficiency $\Delta\lambda/\Delta d$ (d: the length of the air gap), we found that the reflection at the interface between the air gap and the semiconductor with active region should be reduced [14]. Our proposed structure has an Al_xO_y anti-reflection layer at the interface. The refractive index of Al_xO_y is about 1.5 which is close to that of a perfect AR coating. The proposed structure leads not only the enhancement of wavelength tuning characteristics but also the increase in temperature range of athermal operations. This is because tuning efficiency $\Delta\lambda/\Delta L$ can become nearly constant against the air-gap changes by inserting the Al_xO_y layer. This characteristic also enhances the precise control of the wavelength trimming.

3. Wavelength trimming by post-process etching of the cantilever

If a GaAs sacrificial layer is selectively etched to form the air-gap, the released cantilever end shows the upward stress-induced displacement. This displacement is determined by the cantilever structure

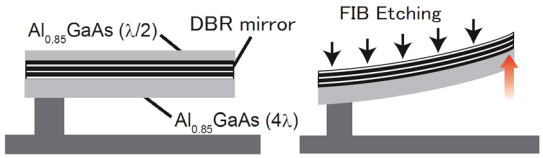

Fig. 2: The schematic of wavelength trimming with surface etching of the cantilever arm.

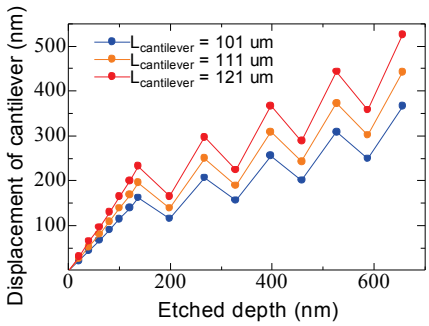

Fig. 3: Calculated displacement of the cantilever as a function of etched depth.

and is given by

$$\Delta d = \frac{3 \cdot t_{DBR} \cdot t_{scl} \cdot L_{cantilever}^{\ 2} \cdot \varepsilon(\Delta a)}{(t_{DBR} + t_{scl})^3} \qquad (1)$$

where t_{DBR} is the thickness of DBR, t_{scl} is the thickness of the strain control layer, $L_{cantilever}$ is the length of the cantilever, Δa is the difference of lattice constants of DBR and the strain control layer and ε is the stress induced by lattice mismatch. The displacement can be changed by modifying the cantilever structure using the post-process FIB etching technique.

Figure 2 shows the schematic of post-process etching for "wavelength trimming". The left and right figures show the cantilever before and after FIB etching respectively. We have about 135 nm-thick $Al_{0.85}Ga_{0.15}As$ layer at the top of DBR mirror for etching protection. When the arm of a cantilever is etched to reduce the thickness of DBRs, the stress-induced displacement is increased due to the increased vertical asymmetry. The upward displacement results in the red-shift due to the increased the air-gap. We calculated the displacement of the cantilever as a function of the etched depth as shown in Fig. 3. While the top $Al_{0.85}Ga_{0.15}As$ layer is etched, the displacement is increased monotonically with the etched depth. If we continue to etch DBR layer, the displacement periodically changes with a period of one DBR pair. This is because average Al composition of DBR layer changes with the etched depth. Despite the periodic change, the figure

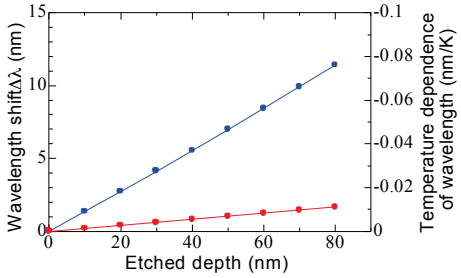

Fig. 4: Calculated wavelength shift and temperature dependence of wavelength as a function of etched depth.

indicates that we can increase the displacement of the cantilever by thinning DBR layer. An etched depth of 100 nm of DBR layer gives us a displacement of above 110 nm and a wavelength shift of about 10 nm if we assume tuning efficiency $\Delta\lambda/\Delta d$ is 0.088. The amount of this shift indicates that etching of the top $Al_{0.85}Ga_{0.15}As$ layer is sufficient for wavelength trimming that we propose.

The temperature dependence of wavelength $\Delta\lambda/\Delta T$ also should be considered when the wavelength trimming is carried out. Our proposed VCSELs with a thermally actuated cantilever enable us to control $\Delta\lambda/\Delta T$ by means of differences of thermal expansion coefficients between DBR layer and the strain control layer. Therefore $\Delta\lambda/\Delta T$ depends on the cantilever structure. If we etch DBR layer for their wavelength trimming, the displacement caused by temperature changes $\Delta d/\Delta T$ may break out the athermal condition. We calculated how the wavelength trimming effects on the athermal operation as shown in Fig. 4. We assumed a 120 μm-long cantilever for athermal operation. As the wavelength is shifted from initial one with the reduced thickness, the temperature dependence of wavelength $\Delta\lambda/\Delta T$ is increased from the athermal operation. If we allow $\Delta\lambda/\Delta T$ to be 0.007nm/K (10 times smaller than conventional VCSELs), we can get a wavelength shift of above 7 nm with such a small $\Delta\lambda/\Delta T$.

4. Fabrication Process

Figure 5 shows the fabrication process. The process includes the formation of a cantilever structure, VCSEL mesa etching, the oxidation process which forms oxide confinement and anti-reflection layer, metal deposition and finally cantilever release by selective etching using citric acid. Cantilever structures and VCSEL mesas were formed by inductively coupled plasma (ICP) dry etching. An Al_xO_y anti-reflection layer can be formed by a lateral wet-oxidation of a 140-nm-thick epitaxial $Al_{0.98}Ga_{0.02}As$ during the formation of oxide apertures for optical and electrical confinement. No extra fabrication process is needed. The small circles, which eventually contain the base of the cantilever, are 20 mm in diameter while the larger bottom mesas are 60 mm in diameter, requiring 25 mm of lateral oxidation. The entire $Al_{0.98}Ga_{0.02}As$ anti-reflection layer was oxidized at 480 °C leaving an unoxidized aperture (~10 μmϕ) at the center of the larger bottom mesa. We used Ni/Ge/Au as a top contact and Au/Zn/Au as a bottom contact [15]. The air-gap is formed by highly selective citric-acid-based chemical etching of a GaAs sacrificial layer underneath the cantilever [16, 17]. After removing the sacrificial layer by selective etching the wafer was dried with boiled acetone in order to avoid a sticking problem. We fabricated a freely suspended 120 x 10 μm^2 cantilever as shown in Fig. 1.

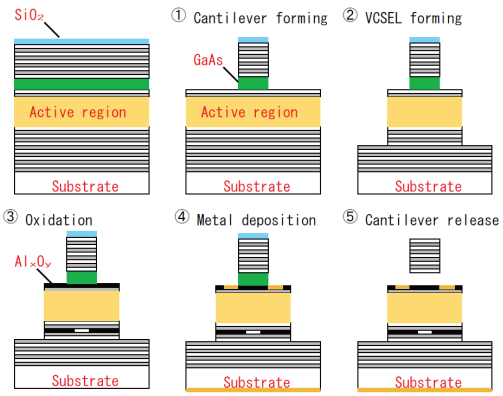

Fig. 5: Fabrication process of athermal 850 nm VCSELs with a thermally actuated cantilever structure.

5. Measurement

We carried out the post-process etching of the cantilever structure to change the displacement for "wavelength trimming". Also, we can obtain the downward displacement by etching the edge of the cantilever without the degradation of mirror reflectivity. This is because the stress relaxation along the cantilever takes place with the stress-induced bending in the perpendicular direction by etching the side of the cantilever end. As a result we can realize both the red-shifted and blue-shifted wavelength changes using the post-process etching

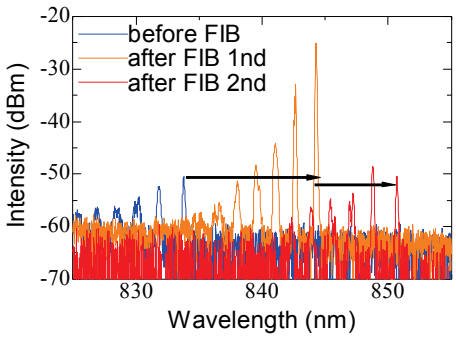

Fig. 6: Measured lasing spectra before and after FIB etching of the arm of the cantilever..

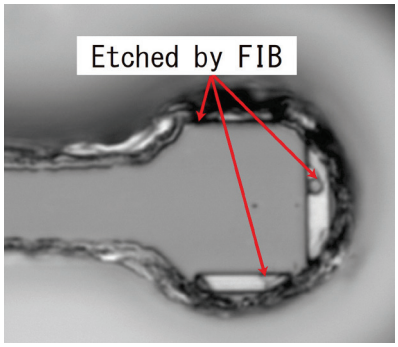

Fig. 7: The SEM top view of an etched cantilever for wavelength trimming.

technique.

We etched the arm of the cantilever by FIB, which leads to the reduction in the thickness. The post-process etching of less than 200 nm results in wavelength shifts of 15 nm. Figure 6 shows the measured spectra before and after two-steps FIB etching. This figure indicates multi-mode operations due to its large oxide aperture, but single-mode operation could be obtained by reducing the oxide aperture size. Output power was changed depending on their resonant wavelengths because its gain or reflectivity is changed. However we expect that we may avoid the changes of laser performances when the wavelength shift is a few nm in practical applications. We realized red-shifts of about 10 nm and 6 nm in the first and second step etching of the cantilever arm, respectively. We also etched the edge of a cantilever end to get blue-shifts. The SEM view of the etched cantilever is shown in Fig. 7. Etched depth was about 550 nm, which corresponds to 4.5 pairs of DBRs. As shown in Fig. 8, the lasing wavelength was blue-shifted by the post-process etching. These results indicate that we can make post-process wavelength control either with red-shift and blue-shift by choosing the etching area of the cantilever structure.

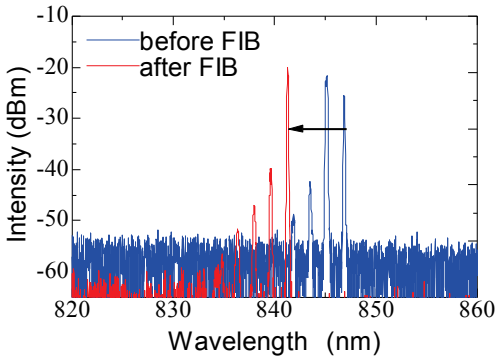

Fig. 8: Measured lasing spectra before and after FIB etching of the edge of the cantilever.

6. Conclusions

We proposed and demonstrated the wavelength trimming of MEMS VCSELs for post-process precise wavelength allocation. We realized both red-shift and blue-shift wavelength changes by choosing the etching area of the cantilever. The proposed concept would be useful for precise wavelength engineering of athermal MEMS VCSELs.

References

[1] C. J. Chang-Hasnain: IEEE J. Sel. Top. Quantum Electron. **6** (2000) 978.

[2] M. C. Y. Huang, K. B. Cheng, Y. Zhou, A. P. Pisano, and C. J. Chang-Hasnain: IEEE J. Sel. Top. Quantum Electron. **13** (2007) 374.

[3] J. Boucart, R. Pathak, D. Zhang, M. Beaudoin, P. Kner, D. Sun, R. J. Stone, R. F. Nabiev, and Wupen Yuen: IEEE Photonics Technol. Lett. **15** (2003) 1186.

[4] C. K. Kim, M. L. Lee, and C. H. Jun: IEEE Photonics Technol. Lett. **16** (2004) 1894.

[5] C. Prott, F. Romer, E. O. Ataro, J. Daleiden, S. Irmer, A. Tarraf, and H. Hillmer: IEEE J. Sel. Top. Quantum Electron. **9** (2003) 918.

[6] M. Lackner, M. Schwarzott, F. Winter, B. Kogel, S. Jatta, H. Halbritter, and Peter Meissner: Opt. Lett. **31** (2006) 3170.

[7] T. Amano, F. Koyama, N. Nishiyama, and K. Iga: IEEE Photonics Technol. Lett. **12** (2000) 510.

[8] T. Amano, F. Koyama, T. Hino, M. Arai, and A. Matsutani: J. Lightwave Techonol. **21** (2003) 596.

[9] N. Nishiyama, C. Caneau, G. Guryanov, X. S. Liu, M. Hu, and C. E. Zah: Electron. Lett. **39** (2003) 437.

[10] W. Janto, K. Hasebe, N. Nishiyama, C. Caneau, T. Sakaguchi, A. Matsutani, F. Koyama, and C. E. Zah: presented at 20th Int. Semiconductor Laser Conf. (ISLC2006), 2006.

[11] H. Sano, A. Matsutani, and F. Koyama, Appl. Phy. Express, 2, (2009), 072101.

[12] H. Sano, and F. Koyama, IEICE ELEX, Vol.6, No. 20, pp.883-888, 2009.

[13] T. Amano, F. Koyama, N. Nishiyama, A. Matsutani, and K. Iga, presented at Conf. on Lasers and Electro-Optics (CLEO2000), 2000.

[14] M. Maute, B. Kogel, G. Bohm, P. Messner, and M. C. Amann: IEEE Photonics Technol. Lett. **18** (2006) 688.

[15] H. R. Kawata, T. Oku, A. Otsuki, and M. Murakami: J. Appl. Phys. **75** (1994) 2530.

[16] M. C. Y. Huang, Y. Zhou, and C. J. Chang-Hasnain: Opt. Express **15** (2007) 1222.

[17] J. H. Kim, D. Ho Lim, and G. M. Yang: J. Vac. Sci. Technol. B **16** (1998) 558.